

# BASIC AND TRANSLATIONAL—ALIMENTARY TRACT

## N-methyl D-Aspartate Channels Link Ammonia and Epithelial Cell Death Mechanisms in *Helicobacter pylori* Infection

JI HYE SEO,\* JAMES G. FOX,‡ RICHARD M. PEEK Jr,§ and SUSAN J. HAGEN\*

\*Department of Surgery, Beth Israel Deaconess Medical Center, Boston, Massachusetts; ‡Division of Comparative Medicine, Massachusetts Institute of Technology, Cambridge, Massachusetts; and §Division of Gastroenterology, Vanderbilt University Medical Center, Nashville, Tennessee

**See editorial on page 1967.**

**BACKGROUND & AIMS:** *Helicobacter pylori* infection is a risk factor for gastric cancer. Ammonia/ammonium (A/A) is a cytotoxin generated by *H pylori* that kills gastric epithelial cells. We investigated whether A/A cytotoxicity occurs by activating N-methyl D-aspartate (NMDA) channels, which results in Ca<sup>2+</sup> permeation and epithelial cell death. **METHODS:** Gastric epithelial cells were cultured to confluence and then incubated with A/A and NMDA channel or cell signaling antagonists. Cells were incubated with wild-type *H pylori* or mutant strains that do not produce A/A. Changes in intracellular Ca<sup>2+</sup> were examined in living cells by confocal microscopy. Biochemical and histochemical techniques were used to examine the relationship between A/A-induced cell death and intracellular levels of Ca<sup>2+</sup>. **RESULTS:** A/A increased Ca<sup>2+</sup> permeation in gastric epithelial cells; the increase was blocked by NMDA receptor and cell signaling antagonists. Wild-type, but not mutant *H pylori*, also caused extensive Ca<sup>2+</sup> permeation of gastric epithelial cells, which was blocked when NMDA-receptor expression was repressed. Ca<sup>2+</sup> that entered cells was initially cytoplasmic and activated proteases. Later, the Ca<sup>2+</sup> was sequestered to cytoplasmic vacuoles that are dilatations of the endoplasmic reticulum. Inositol-3-phosphate-dependent release of Ca<sup>2+</sup> from the endoplasmic reticulum and protease activity damaged mitochondria, reduced levels of adenosine triphosphate, and transcriptionally up-regulated cell death effectors. Expression of the NMDA receptor was altered in stomachs of mice infected with *H pylori*. **CONCLUSIONS:** A/A affects gastric epithelial cell viability by allowing excessive Ca<sup>2+</sup> permeation through NMDA channels. NMDA channels might thereby regulate cell survival and death pathways during development of gastric cancers associated with *H pylori* infection.

**Keywords:** Stomach Cancer; Apoptosis; Tumorigenesis; Calcium; Inositol-3-Phosphate Signaling.

Infection with *Helicobacter pylori* (HP) occurs in 50% of the world's population and is a major risk factor for gastric cancer development. Gastric cancer is 5.5% of the global cancer burden and is the second most common cause of cancer deaths worldwide.<sup>1,2</sup> HP express a number of virulence factors including members of the *cag* pathogenicity island, *vacA* producing vacuolating cytotoxin, lipopolysaccharide, and ammonia/ammonium (A/A), which individually or together are thought to facilitate cancer development. The *ure* genes of HP are required for expression of urease, which facilitates the production of A/A from urea in the gastric juice.<sup>3</sup> HP also express enzymes that hydrolyze asparagine and glutamine, further increasing A/A production.<sup>4,5</sup> A/A production is essential for HP colonization and persistence of infection,<sup>6</sup> but is cytotoxic to gastric epithelial cells.

The concentration of A/A in gastric juice is normally 0.5–0.7 mmol/L but can increase to more than 20 mmol/L in patients infected with HP.<sup>7,8</sup> When cultured human gastric cells are incubated with urease-positive HP and urea, about 20 mmol/L A/A is generated in 2 hours and 40 mmol/L is generated in 24 hours and the viability of cells is reduced as the A/A concentration increases.<sup>9</sup> In vivo<sup>10,11</sup> and in vitro<sup>12–14</sup> studies have confirmed that A/A, per se, also reduces the viability of gastric epithelial cells. Two hypotheses have been suggested to explain the effects of A/A on gastric epithelial cells. First, A/A generated by urease in the presence of urea rapidly increases intracellular pH, which elicits an associated brief spike of intracellular Ca<sup>2+</sup> that was shown to be derived from intracellular stores.<sup>15</sup> The lipid solubility of ammonia allows it to enter cells, resulting in an increase in intracellular pH.<sup>16</sup> Alternatively, it was suggested that A/A accelerates the

**Abbreviations used in this paper:** A/A, ammonia/ammonium; 2-APB, 2-aminoethoxydiphenyl borate; ATP, adenosine triphosphate; cAMP, cyclic adenosine monophosphate; ER, endoplasmic reticulum; HP, *Helicobacter pylori*; NMDA, N-methyl D-aspartate; RGM1, rat gastric mucosal 1; NR2B, N-methyl D-aspartate receptor subunit 2B; PKA, protein kinase A; Rh, Rhodamine; *ureB*, urease subunit B gene; wkPI, weeks post-infection.

conversion of glutamine to glutamate by glutamine synthetase, which depletes cells of adenosine triphosphate (ATP) and reduces cell viability.<sup>17</sup> It is not fully understood why the viability of many cancer-derived epithelial cells is not affected by A/A when compared with non-transformed cells incubated with the same dose and time.<sup>18–20</sup> Thus, we asked whether specific mechanisms exist to render nontransformed epithelial cells susceptible to ammonia cytotoxicity that are modified in gastric cancer.

*N*-methyl D-aspartate (NMDA) channels in neurons are heterotetramers consisting of NR1 and NR2 (2A–2D) subunits, which serve as glutamate-gated ion channels that transport Ca<sup>2+</sup>.<sup>21,22</sup> A/A is thought to activate NMDA channels in neurons by depolarizing the cell membrane, which increases NMDA channel-mediated Ca<sup>2+</sup> permeation in the absence of receptor agonists, such as glutamate and glycine.<sup>23</sup> Neuronal cell death occurs when A/A is in high concentration because Ca<sup>2+</sup> permeation through NMDA channels occurs at nonphysiological rates.<sup>23</sup> Because gastric cells are exposed to high A/A concentrations in HP infection, our aim was to determine if A/A-induced NMDA channel activation regulates Ca<sup>2+</sup> permeation and epithelial cell death in gastric cells that can be blocked by NMDA channel antagonists. NMDA channel subunits are transcriptionally down-regulated in gastric cancer and in many gastric cancer cell lines,<sup>24</sup> suggesting that transformed cells would be less responsive to A/A while it rapidly kills nontransformed cells in a dose-dependent manner. This work may thus provide important insights into how HP infection affects apoptosis rates to support cancer development *in vivo*.

## Materials and Methods

### Cell Culture, Transfection, and Incubation With HP

Rat gastric mucosal 1 (RGM1) cells were cultured and experiments were performed in standard buffer as described previously.<sup>13</sup> MKN28 cells were cultured and then incubated with the cag+ toxigenic HP strain 60190 or its isogenic urease subunit B gene (*ureB*) mutant as described by Wroblewski et al.<sup>19</sup> Cultured cells were plated on 35-mm culture dishes with an affixed cover glass (Matteck, Ashland, MA) for live cell microscopy studies.

MKN28 cells were transfected with a control or NMDAR2B-pDP3 expression plasmid (kindly provided by Dr. John Woodward, Medical University of South Carolina) with FuGENE 6 as described by Liu et al.<sup>24</sup> Transfection efficiency was 53.9% ± 0.3% (n = 3). Cells were used 2 days after transfection. Experiments with MKN28 cells and HP were performed for 48 hours in RPMI media without antibiotics but containing 10% serum.

### Live-Cell Microscopy

Studies in living cells were performed using a Zeiss LSM510 Meta laser scanning confocal system (Carl Zeiss, Inc., Thornwood, NY) outfitted with a Life Imaging Services (Reinach, Switzerland) Cube and Box incubator chamber and O<sub>2</sub> and CO<sub>2</sub> control using specific probes. The details of the laser con-

figurations, probes, and post-acquisition image processing are reported in the Supplementary Materials and Methods.

### Western Blots

After experiments, Western blots of RGM1 cells were prepared as described previously.<sup>25</sup> Filters were incubated with anti-*N*-methyl D-aspartate receptor subunit 2B (NR2B) (Alomone Labs, Jerusalem, Israel), anti-Bcl-2-associated X protein (BAX; BD Pharmingen, San Jose, CA), or anti-Bcl-2 homologous antagonist killer BAK (BAK; Santa Cruz, Santa Cruz, CA). The filter was stripped and re-probed with a β-actin antibody (Sigma-Aldrich, St. Louis, MO). The resulting bands were quantified using ImageJ (National Institutes of Health, Bethesda, MD) with the β-actin band used to normalize loading.

### Immunohistochemistry

RGM1 cells were fixed in 4% formaldehyde and then stained with anti-cytochrome *c* oxidase subunit 1 (Invitrogen, Carlsbad, CA) or with anti-NR2B antibody (Abcam, Cambridge, MA) and the resulting images were quantified as reported in the Supplementary Materials and Methods section.

Paraffin sections from control or HP-infected mice were stained using an anti-NR2B antibody (Abcam). For co-localization studies, anti-intrinsic factor (a kind gift from Dr David Alpers, Washington University, St. Louis, MO) staining was performed to localize chief cells, and *Dolicho biflorus* agglutinin (Invitrogen) was used to localize parietal cells. Archived tissues were used at 6, 12, or 20 weeks post-infection (wkPI) from C57BL/6 mice (female) infected with HP as described previously.<sup>25,26</sup>

### Cell Viability

The viability of RGM1 cells was evaluated by a colorimetric assay using crystal violet as described previously.<sup>13</sup>

### ATP and Proteases

ATP was measured with the CellTiter-Glo kit (Promega, Madison, WI) in cells incubated for 120 minutes with 20 mol/L NH<sub>4</sub>Cl at pH 7.4 with or without inhibitors. Calpain and cathepsin B activation was measured in cells at 0, 10, 30, 60, and 120 minutes after the addition of 20 mmol/L NH<sub>4</sub>Cl at pH 7.4 with or without 2S,3S-trans-(Ethoxycarbonyloxirane-2-carbonyl)-L-leucine-(3-methylbutyl) amide E64d (2E64d, 10 μmol/L; Biomol, Plymouth Meeting, PA), a calpain and cathepsin B inhibitor, using specific kits (Invitrogen).

### Statistics

Results are expressed as mean ± standard error of the mean and were analyzed using SigmaStat software (SPSS, Inc, Chicago, IL). Data with a single treatment were analyzed by one-way analysis of variance. Data to compare differences in multiple treatments over time were analyzed by 2-way analysis of variance. The Student-Neuman-Keuls post hoc test was used to determine differences between means. If variances were not normally distributed, the analysis was performed on ranks.

## Results

### NMDA Channel Activation Occurs After Exposure to NH<sub>4</sub>Cl or HP-Generated A/A to Induce Ca<sup>2+</sup>-Permeation in Gastric Epithelial Cells

Immediately after the addition of A/A to RGM1 cells, there was a weak and diffuse fluo-3 fluorescence signal in the

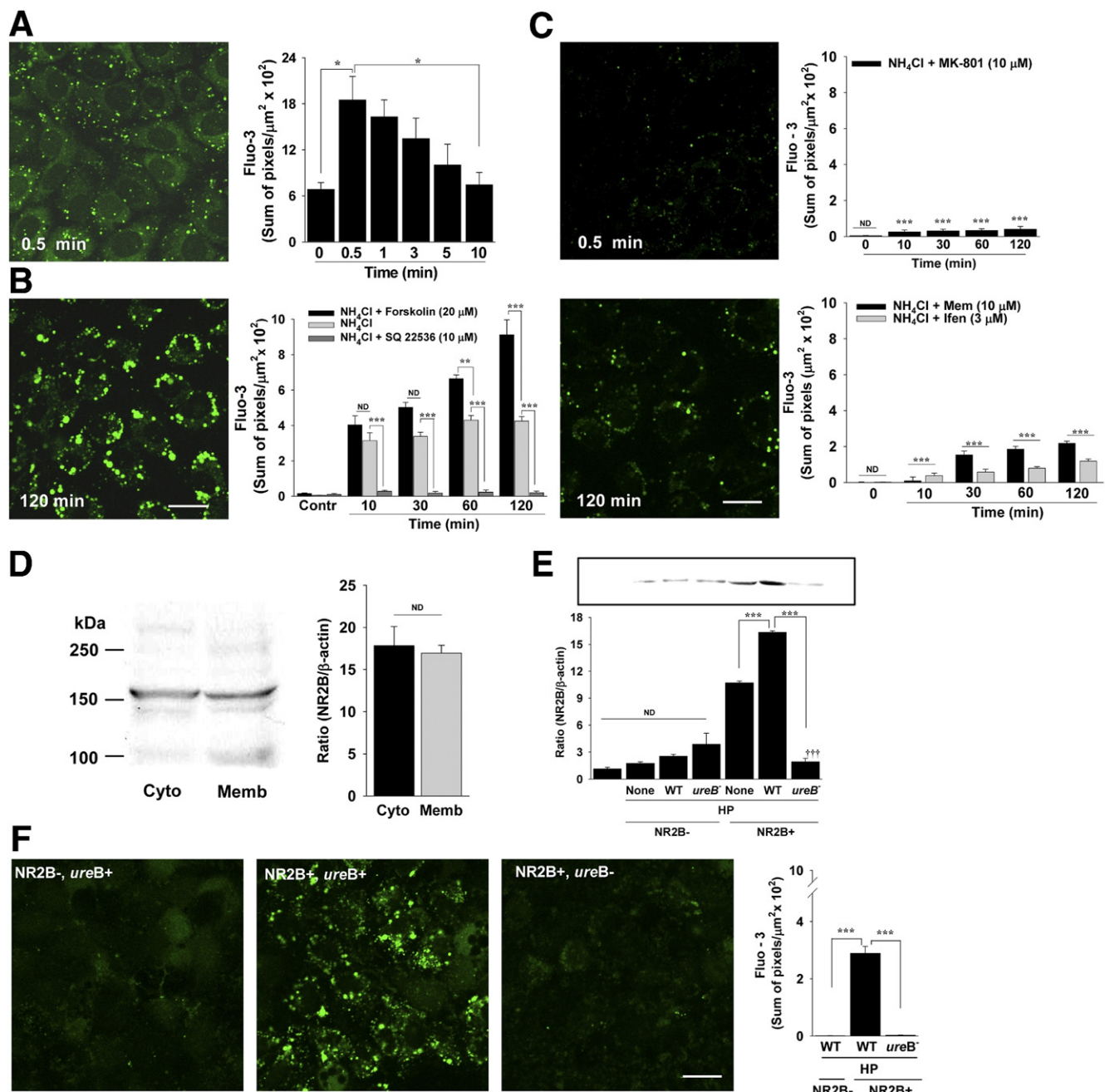


**Figure 1.**  $\text{Ca}^{2+}$  influx during A/A exposure occurs by NMDA channel activation in gastric epithelial cells. (A) Fluorescence and quantification of cytoplasmic fluo-3 signal after the addition of A/A. n = 3; \*P < 0.05 compared with 0.5 minutes. (B) Fluorescence and quantification of fluo-3 signal in vacuoles in the presence of A/A. Fluo-3 in vacuoles also was measured with forskolin, which increases cAMP, and with SQ 22536, which is a cAMP antagonist. Control (Contr) are cells imaged with vehicle, forskolin, or SQ without A/A. n ≥ 7; \*\*P < .01, \*\*\*P < .001. ND, not different. Comparisons are as indicated by brackets. (A and B) Scale bar, 20  $\mu\text{m}$ . (C) Fluorescence and quantification of fluo-3 signal in vacuoles with A/A and MK-801, Memantine (Mem), or ifenprodil (Ifen). n = 3; \*\*\*P < .001. ND, not different. Comparisons with time-matched data for A/A in B. Scale bar, 20  $\mu\text{m}$ . (D) Western blot and quantification of NR2B in membrane-associated (Membr) or cytosolic (Cyto) fractions of RGM1 cells as a ratio of band density to  $\beta$ -actin. (E) Western blot and quantification of NR2B in whole-cell extracts from native MKN28 cells, MKN28 cells transfected with the control plasmid (NR2B-), or MKN28 cells transfected with the NMDAR2B expression plasmid (NR2B+) and incubated without (None) or with wild-type (WT) HP or its isogenic ureB mutant (ureB-). n = 2 different sets of transfected cells; \*\*\*P < .001. ND, not different. Comparisons are as indicated by brackets. +++P < .001 compared with both None and WT cells incubated with HP. (F) Fluorescence and quantification of fluo-3 signal from MKN28 cells without (NR2B-) or with NR2B (NR2B+) expression at 48 hours after incubation with WT (ureB+) or mutant (ureB-) HP as described in E. n = 2 different sets of transfected cells; \*\*\*P < .001. Comparisons are as indicated by brackets. Scale bar, 20  $\mu\text{m}$ .

cytoplasm that peaked and then decreased to control levels by 10 minutes (Figure 1A). The fluo-3 signal also was detected in a vacuolar compartment that expanded significantly ( $P < .001$ ) in size (perimeter of  $3.56 \pm 0.73 \mu\text{m}$  at 0.5

min to  $6.67 \pm 0.73 \mu\text{m}$  at 120 min; n = 7), and intensity (Figure 1A and B) over time. The sum of fluo-3 signal in vacuoles increased from 10 to 120 minutes in the presence of A/A alone (Figure 1B), but could be amplified significantly in

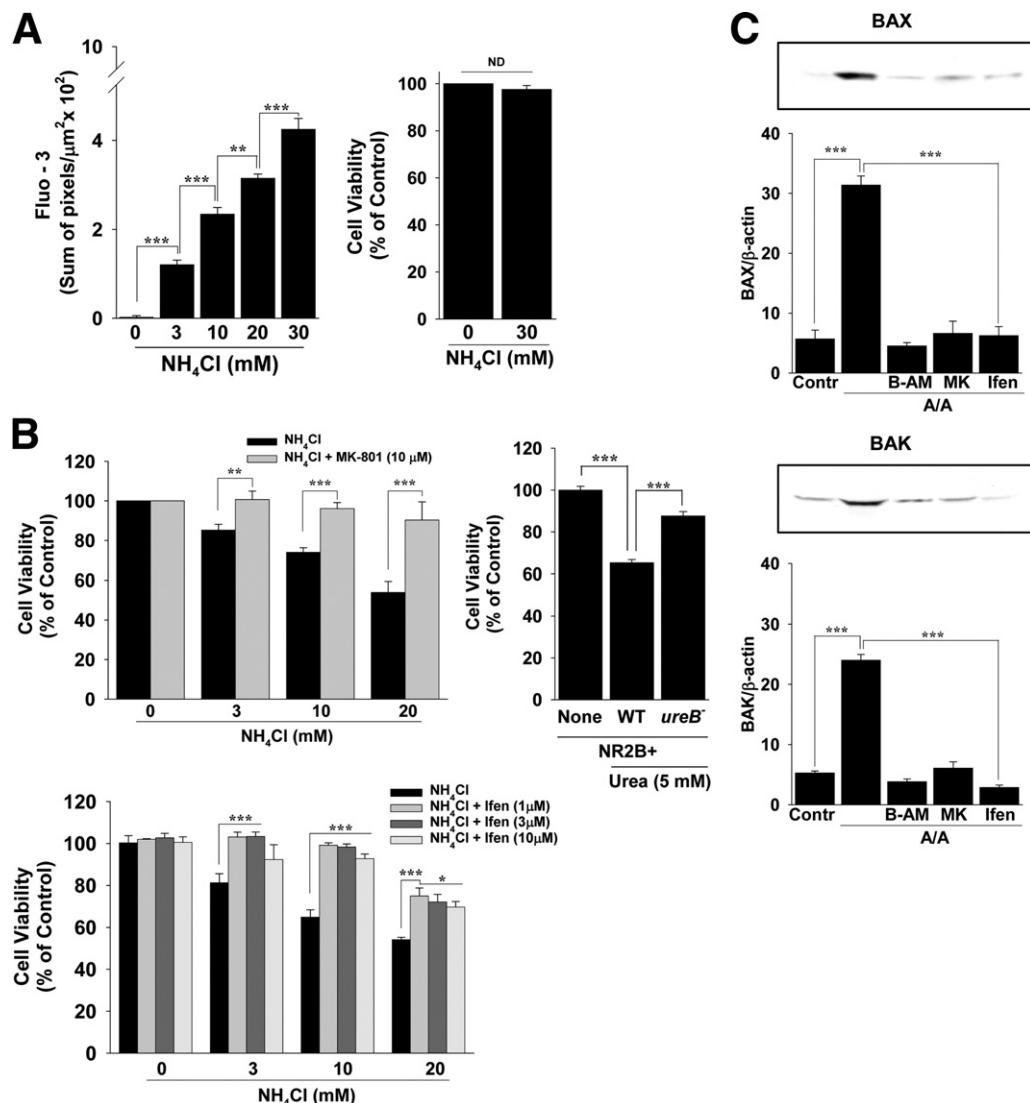


**Figure 2.** Long-term (24 h) A/A-induced NMDA channel activation reduced cell viability and regulated the transcription of apoptosis genes. (A) Quantification of fluo-3 signal in vacuoles at 120 minutes. At the end of microscopy experiments, cell viability was measured. (B) Cell viability at 24 hours with A/A and MK-801 or ifenprodil (Ifen). MKN28 cells were transfected with the NMDAR2B expression plasmid (NR2B+) and incubated without HP (None) or with 5 mmol/L urea and wild-type (WT) HP or its isogenic *ureB*<sup>-</sup>. (C) Cells were incubated with A/A and BAPTA-AM (B-AM), MK-801 (MK), or ifenprodil (Ifen). Band intensity for BAX or BAK was quantified as a ratio to β-actin. n ≥ 3 experiments per condition; \*P < .05, \*\*P < .01, \*\*\*P < .001. ND, not different. Comparisons as indicated by brackets.

the presence of forskolin, which increases cyclic adenosine monophosphate (cAMP) (Figure 1B). Likewise, fluo-3 signal in vacuoles with A/A exposure (no forskolin) was attenuated to near-control levels when cAMP was blocked with SQ 22536 (Figure 1B).

MK-801, a selective and high-affinity NMDA-receptor antagonist, has been used extensively to block NMDA channel activation in vitro and in vivo in animal models.<sup>24,27-29</sup> We thus used MK-801 to show that the intracellular Ca<sup>2+</sup> signal with A/A exposure was caused by extracellular Ca<sup>2+</sup> permeation through NMDA channels. When cells were exposed to A/A in the presence of MK-801, the initial diffuse calcium signal and the bright fluorescence in vacuoles was attenuated significantly (Figure 1C). Likewise, the NMDA channel antagonist Memantine (Namenda, TOCRIS, Ellisville, MO) and the highly

specific NR2B subunit antagonist ifenprodil blocked the initial cytoplasmic signal (not shown) and bright fluorescence in vacuoles (Figure 1C). The NR2B-receptor subunit of NMDA channels is found in both cytoplasmic and membrane-associated compartments in RGM1 cells, as shown in Western blots (Figure 1D). The molecular weight of NR2B in brain is about 166 kilodaltons and we see a strong band at that molecular weight in RGM1 cells (Figure 1D). Immunostaining of nonpermeabilized RGM1 cells showed that NR2B subunits are expressed in the apical cell cytoplasm and are localized to the apical, rather than basolateral, surface (Supplementary Figure 1).

To determine if HP infection also results in A/A-induced Ca<sup>2+</sup> permeation through NMDA channels, we used human MKN28 gastric cancer epithelial cells incubated with wild-type HP strain 60190 or its isogenic *ureB*<sup>-</sup>

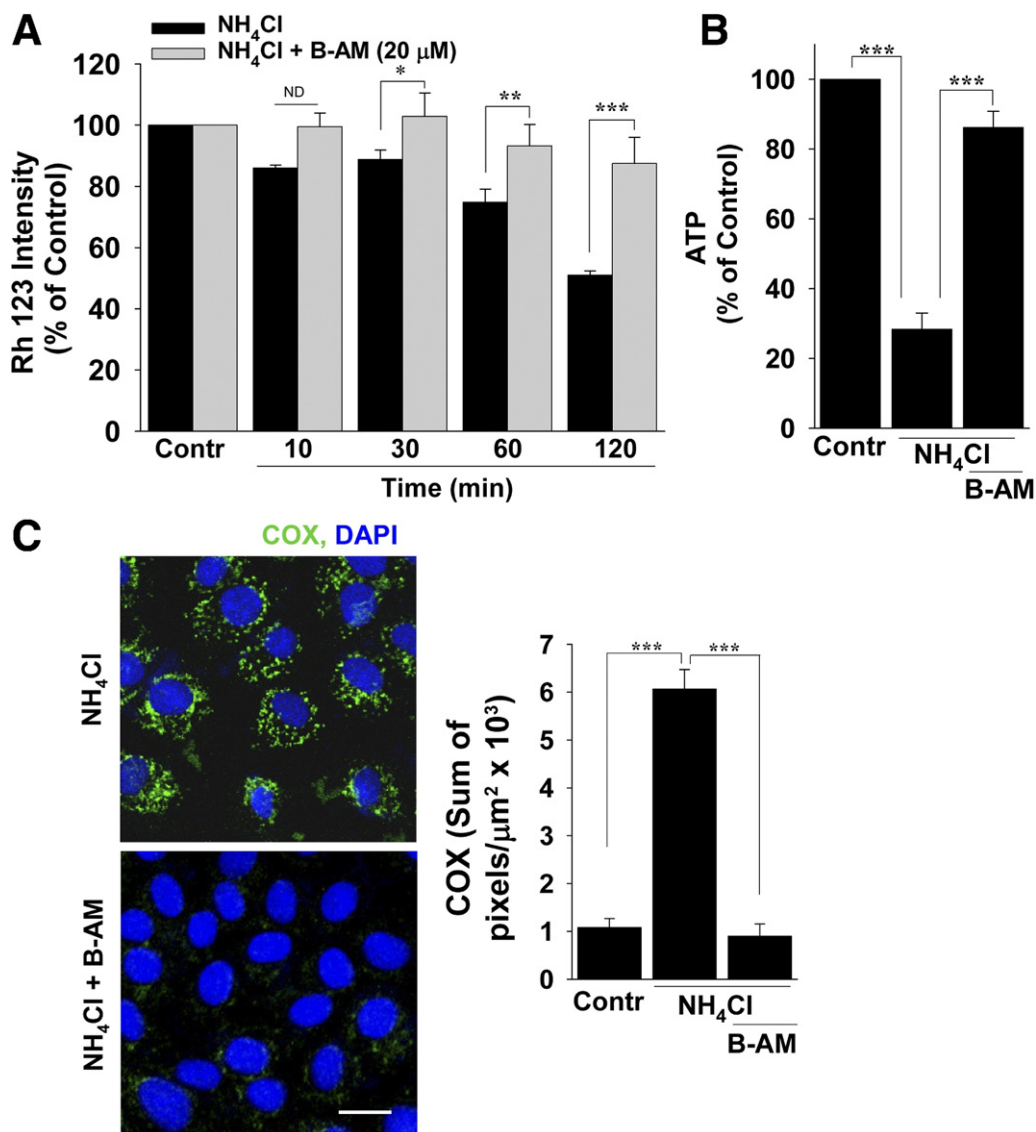


**Figure 3.** Ca<sup>2+</sup> from A/A-induced NMDA channel activation structurally and functionally damages mitochondria. (A) Untreated (live) RGM1 cells were incubated with Rh 123 to measure mitochondrial membrane potential (Contr). Membrane potential also was measured for 10–120 minutes during A/A exposure (NH<sub>4</sub>Cl) with or without BAPTA-AM (B-AM). (B) At the end of the experiment in A, ATP was measured or (C) cells were lightly fixed and incubated with anti-cytochrome c oxidase 1 (COX) (green). n ≥ 3; \*P < .05, \*\*P < .01, \*\*\*P < .001. ND, not different. Comparisons as indicated by brackets. Scale bar, 20 μm.

mutant. Because MKN28 cells transcriptionally down-regulate NR2B but express all other NMDA-receptor subunits,<sup>30</sup> we transfected cells with an NR2B expression plasmid that significantly increased NR2B protein expression (Figure 1E). When NR2B- cells were incubated with wild-type HP (*ureB* +), there was virtually no fluo-3 signal (Figure 1F). In contrast, NR2B+ cells incubated with wild-type HP (*ureB* +) showed significant fluo-3 fluorescence in an intracellular compartment (Figure 1F), identical to the results with AA alone. In addition, these cells also showed a significant increase in NR2B protein expression (Figure 1E). Results with NR2B+ cells incubated with the HP *ureB*- mutant showed a significant attenuation of Ca<sup>2+</sup> permeation through NMDA channels (Figure 1F). This mutant also blocked the plasmid-induced expression of NR2B (Figure 1E).

#### NMDA Channel Activation Reduces Cell Viability During A/A Exposure

Ca<sup>2+</sup> permeation into vacuoles increased dose-dependently from 3 to 30 mmol/L NH<sub>4</sub>Cl but this increase in Ca<sup>2+</sup> had no effect on cell viability at 120 minutes (Figure 2A). Long term (24 h), however, A/A dose-dependently reduced cell viability in RGM1 cells (Figure 2B) as did A/A produced in 48 hours from urea in the presence of wild-type HP but not *ureB*- mutant HP in NR2B+ MKN28 cells (Figure 2B). This reduction in cell viability with up to 20 mmol/L NH<sub>4</sub>Cl could be reversed with the NMDA channel antagonists MK-801 or ifenprodil (Figure 2B), or significantly improved with Memantine (not shown). Because A/A reduces cell viability by activating apoptosis in RGM1 cells,<sup>13</sup> and BAX and BAK are the

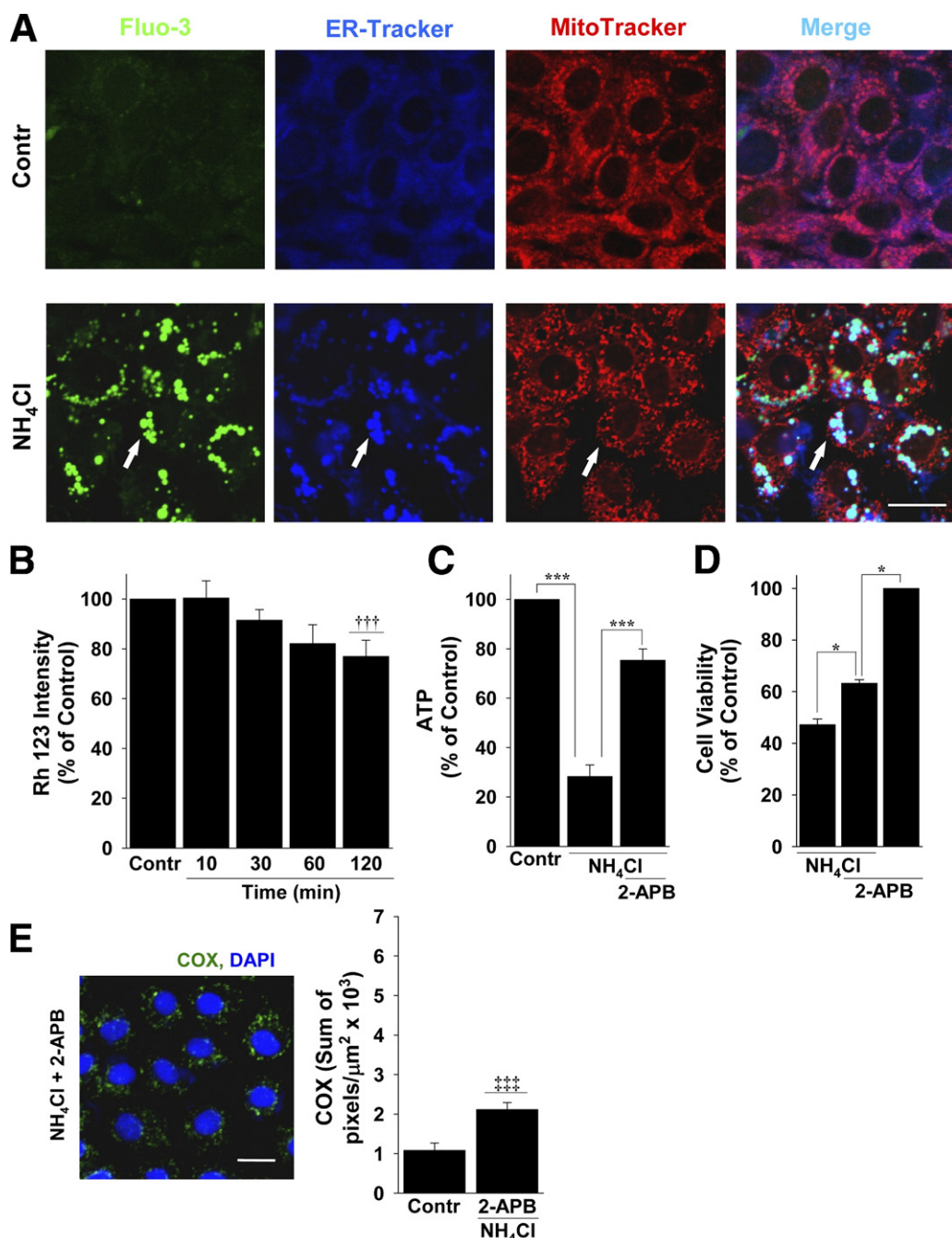


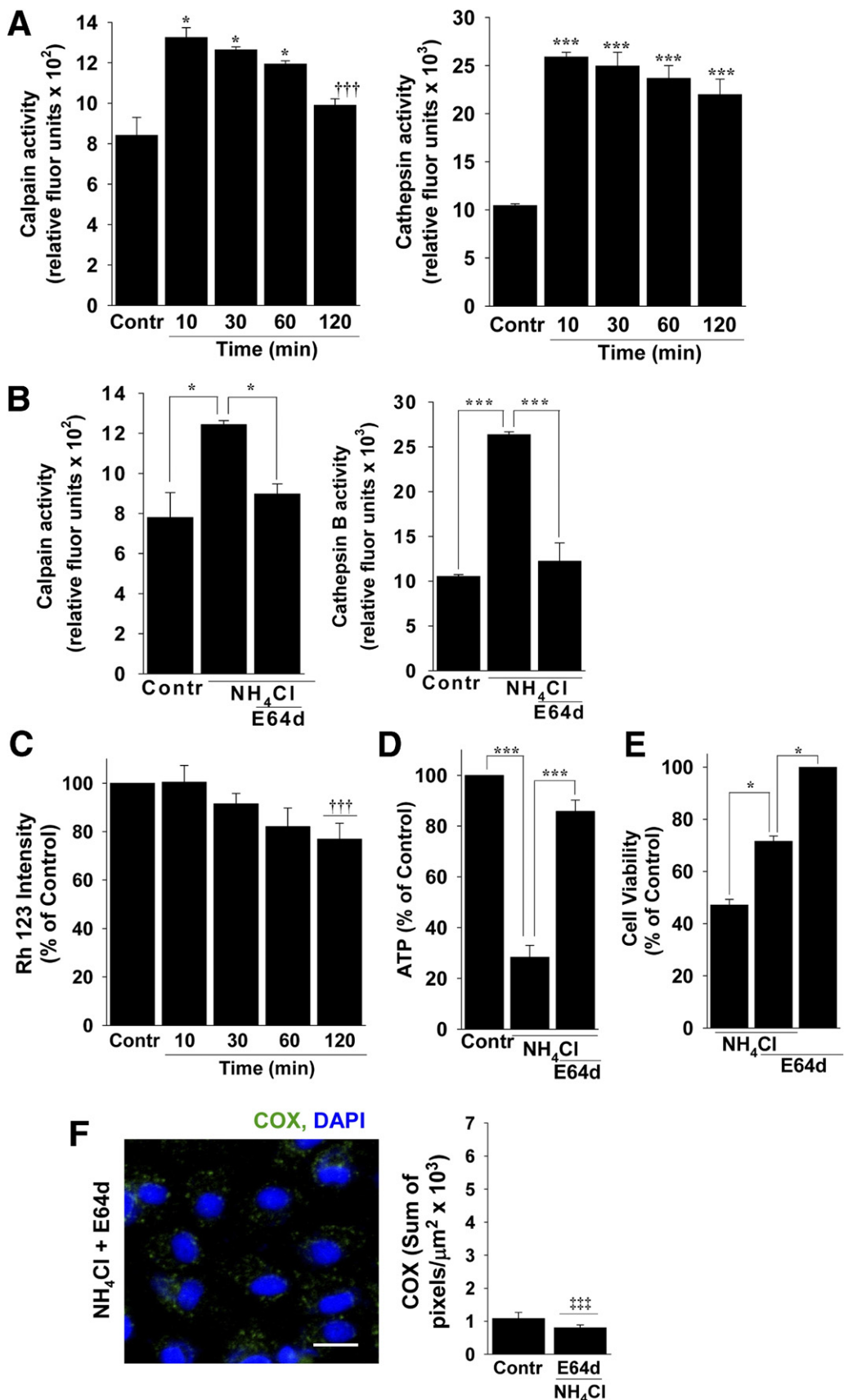
**Figure 4.** A/A-induced NMDA-mediated  $\text{Ca}^{2+}$  localizes to ER and is transferred to mitochondria, causing mitochondrial damage and cell death. (A) Untreated (live) RGM1 cells (Contr) or cells treated with A/A ( $\text{NH}_4\text{Cl}$ ) were incubated simultaneously with Fluo-3 (green), ER-Tracker (blue), and MitoTracker (red) and the merged images (turquoise) were used to examine the co-localization of Fluo-3 with the ER or mitochondria. 2-APB was used to block the transfer of  $\text{Ca}^{2+}$  from ER to mitochondria and the resulting effect this had on (B) mitochondrial membrane potential with Rh 123, (C) ATP production, (D) cell viability, and (E) mitochondrial membrane damage by staining with anti-cytochrome c oxidase 1 (COX) (green) is shown.  $n \geq 3$ ; \* $P < .05$  and \*\*\* $P < .001$ . Comparisons as indicated by brackets. \*\*\* $P < .001$  compared with A/A alone in Figure 3A. # $P < .001$  compared with A/A in Figure 3C. Scale bars, 20  $\mu\text{m}$ .

pro-apoptotic effectors in gastric surface and pit/neck cells,<sup>25</sup> we tested whether A/A-induced NMDAR activation transcriptionally regulates BAX and BAK expression in the presence of A/A (Figure 2C). Although BAX and BAK expression increased more than 6-fold with A/A exposure, this expression was attenuated to control levels or below by buffering intracellular  $\text{Ca}^{2+}$  with 1,2-Bis(2-aminophenoxy)ethane-N,N,N',N'-tetraacetic acid tetrakis(acetoxy-

methyl ester) (BAPTA)-AM or by inhibiting NMDA-receptor activation with MK-801 or ifenprodil (Figure 2C).

#### *$\text{Ca}^{2+}$ Permeation by A/A-Induced NMDA Channel Activation Damages Mitochondria and Reduces Intracellular ATP*

When A/A was added to live cells preloaded with rhodamine (Rh) 123, the fluorescence intensity of Rh 123



was reduced significantly (Figure 3A). Concomitantly, intracellular ATP was also reduced significantly (Figure 3B). The intracellular calcium chelator BAPTA-AM was used to buffer the effects of  $\text{Ca}^{2+}$  permeation during A/A exposure and it not only restored mitochondrial membrane potential (Figure 3A) but improved intracellular ATP (Figure 3B). With A/A exposure, there was bright cytochrome *c* oxidase 1 fluorescence in mitochondria (Figure 3C), and this fluorescence was reduced to control levels by BAPTA-AM (Figure 3C).

#### **A/A-Induced Cytoplasmic Vacuoles are Dilatations of the Endoplasmic Reticulum Containing $\text{Ca}^{2+}$**

To determine if  $\text{Ca}^{2+}$  is taken up by mitochondria or another intracellular compartment, we used live-cell microscopy with RGM1 cells that were incubated with fluo-3 in the presence of both ER-Tracker and Mito-Tracker (Invitrogen, Carlsbad, CA). After the addition of A/A, the endoplasmic reticulum (ER) compartment was vesicular and in the merged images from cells treated with A/A there was co-localization of fluo-3 with ER but not mitochondria (Figure 4A). The incidence of co-localization of ER-Tracker and fluo-3 during A/A exposure was  $78.53\% \pm 1.34\%$  ( $n = 3$ ), with the remaining fluo-3 signal in small vacuoles that were not ER or mitochondria (Figure 4A). Stimulating NMDA channel activation with NMDA and glycine also resulted in fluo-3 accumulation in ER-derived vacuoles that was blocked completely with ifenprodil (Supplementary Figure 2).

Because  $\text{Ca}^{2+}$  was sequestered to the ER, it is possible that damage to mitochondria occurs by the release of ER  $\text{Ca}^{2+}$  to mitochondria in the presence of A/A by inositol-3-phosphate-receptor activation.<sup>31</sup> To test this idea, we pre-incubated RGM1 cells with the inositol-3-phosphate-receptor antagonist 2-APB, incubated cells with A/A in the continued presence of 2-APB, and then measured the mitochondrial membrane potential using Rh 123 in live cells (Figure 4B). The results showed that in contrast to A/A alone (Figure 3A), 2-APB significantly improved the A/A-induced decrement in mitochondrial membrane potential (Figure 4B), reduction in ATP (Figure 4C), cell viability (Figure 4D), and mitochondrial outer membrane damage evaluated by cytochrome *c* oxidase 1 immunolabeling (Figure 4E).

#### **A/A-Induced NMDA Channel Activation Increases $\text{Ca}^{2+}$ -Activated Proteases**

Because the initial intracellular calcium concentration increased significantly after A/A exposure, we exam-

ined the role of  $\text{Ca}^{2+}$ -activated protease on mitochondrial damage and cell viability (Figure 5). Calpain is linked to neurotoxic NMDA-receptor activation<sup>32</sup> and cathepsin B is released from lysosomes to affect mitochondrial function and integrity when intracellular  $\text{Ca}^{2+}$  increases.<sup>33</sup> Immediately after the addition of A/A to cells, both calpain and cathepsin B were activated (Figure 5A). To test whether the level of calpain and cathepsin B activation is sufficient to affect mitochondrial function, we measured mitochondrial membrane potential using Rh 123 with A/A in the presence of E64d, a calpain and cathepsin B inhibitor that effectively reduced the activity of both enzymes to control levels in the presence of A/A (Figure 5B). With E64d, mitochondrial membrane potential improved significantly (compare Figures 5C and 3A). Intracellular ATP (Figure 5D), cell viability (Figure 5E), and mitochondrial permeability to anti-cytochrome *c* oxidase 1 (Figure 5F) also improved significantly by blocking calpain and cathepsin B activity with E64d.

#### **NMDA-Receptor Expression Is Altered in HP Infection In Vivo**

In the in vivo mouse stomach, NR2B-receptor subunits of NMDA channels are highly expressed in gastric parietal cells and are moderately expressed in surface and chief cells (Figure 6A and E). Although the expression of NR2B was present at 6 (Figure 6B and E) and 12 (Figure 6E) wkPI in surface cells most terminally differentiated at the luminal surface, its expression increased significantly at 20 wkPI and was localized along the surface and the length of gastric pits (Figure 6C and E). The same expression pattern was found in the antrum (Supplementary Figure 3). Parietal cells were present in gastric glands at 6 wkPI (Figure 6B, specifically identified in the *D biflorus* agglutinin panel), but NR2B was expressed only minimally in these cells (Figure 6B and E). Instead, NR2B was highly expressed at the base of gastric glands in intrinsic factor-positive chief cells (Figure 6B and E). At 12 (not shown) and 20 wkPI, gastric glands from HP-infected mice with metaplastic cells, which are epithelial precursor cells for gastric cancer,<sup>34</sup> showed little to no NR2B expression (Figure 6C). The immunolocalization of NR2B in gastric tissue sections was specific, as shown by using the NR2B peptide to inhibit (block) antibody binding (Figure 6D).

#### **Discussion**

This study shows that brain-specific NMDA channels are responsible for the cytotoxic effects of A/A on

**Figure 5.** NMDA-induced  $\text{Ca}^{2+}$  permeation activates proteases that contribute to mitochondrial dysfunction during A/A exposure. (A) Calpain and cathepsin B activity in control (Contr) cells or at 10–120 minutes after exposure to 20 mmol/L  $\text{NH}_4\text{Cl}$ .  $n = 3$  experiments per time point; \* $P < .05$  and \*\*\* $P < .001$  compared with control. ††† $P < .001$  compared with 10 minutes. (B) Blockade of calpain and cathepsin B with E64d.  $n = 3$ ; \* $P < .05$ , \*\*\* $P < .001$ . Comparisons as indicated by brackets. Effects of E64d on (C) mitochondrial membrane potential, (D) intracellular levels of ATP, (E) cell viability, and (F) damage to the inner mitochondrial membrane evaluated by staining with anti-cytochrome *c* oxidase 1 (COX) (green) and 4',6-diamidino-2-phenylindole to stain nuclei (blue).  $n \geq 3$  experiments per condition; \* $P < .05$ , \*\*\* $P < .001$ . Comparisons as indicated by brackets. ††† $P < .001$  compared with  $\text{NH}_4\text{Cl}$  alone in Figure 3A. ‡‡‡ $P < .001$  compared with  $\text{NH}_4\text{Cl}$  alone in Figure 3C. Scale bar, 20  $\mu\text{m}$ .

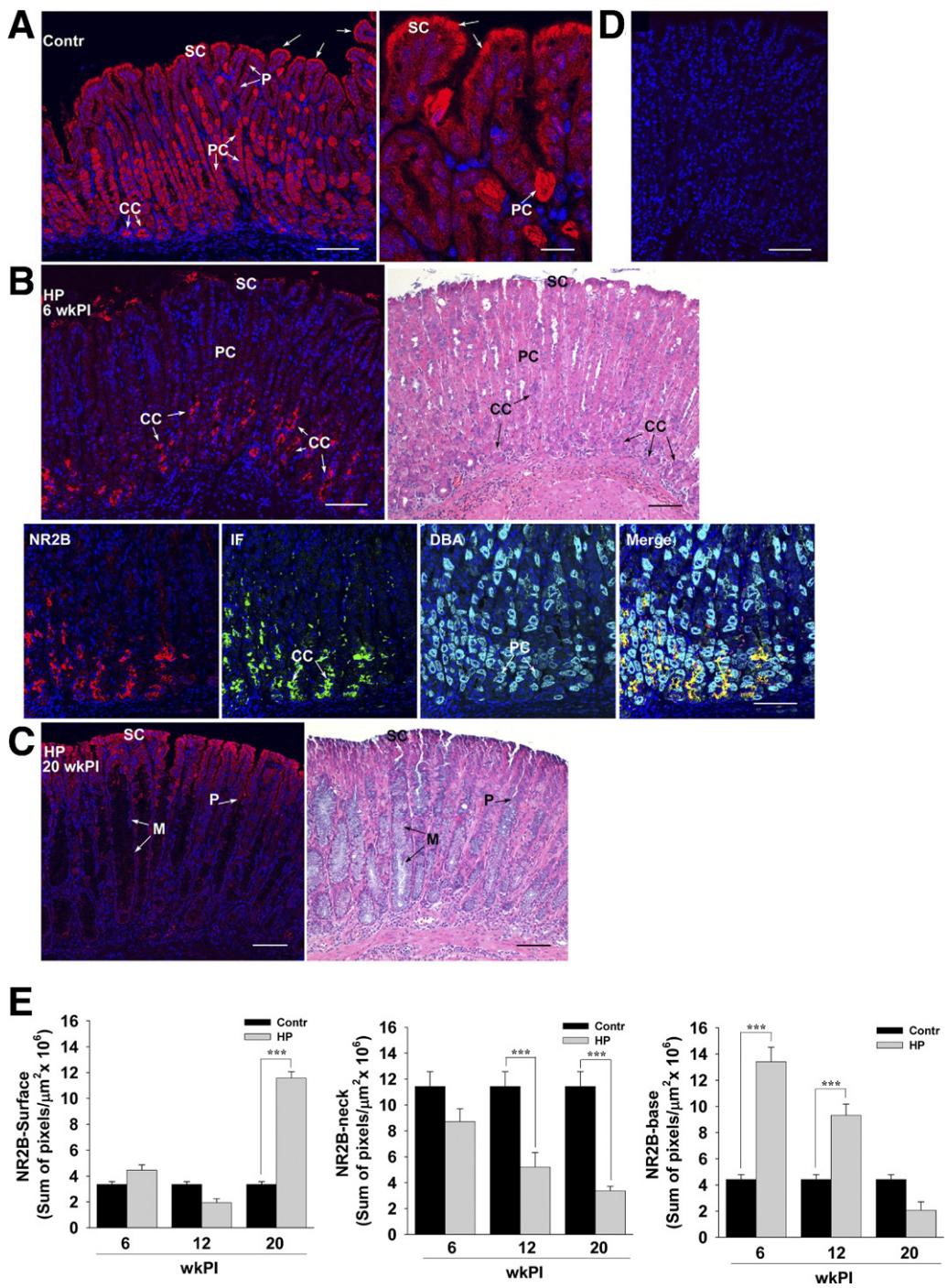


**Figure 6.** NMDA channel subunit NR2B expression in surface, parietal, and chief cells is transcriptionally regulated in HP-infected tissues. Paraffin-embedded tissues from (A) sham- (Contr-20 wkPI) or (B) 6 and (C) 20 wkPI HP-infected mice were stained for the NR2B subunit (red) of NMDA channels, intrinsic factor (IF) to localize chief cells (green), *D. biflorus* agglutinin (DBA) to localize parietal cells (turquoise), and 4',6-diamidino-2-phenylindole to identify nuclei (blue). In B-Merge, co-localization of IF and NR2B is yellow (arrows). (D) A serial section from the tissue in B (6 wkPI HP-infected) was incubated with a 100-fold excess of NR2B peptide to identify nonspecific staining. (B and C) Serial sections also were stained with H&E and included for orientation. (E) Quantification of the sum of fluorescence pixels in tissues from control (Contr) or HP-infected mice at 6, 12, and 20 wkPI.  $n \geq 6$  mice per condition; \*\*\* $P < .001$ ; comparisons as indicated by brackets. CC, chief cells; P, gastric pit; PC, parietal cells; SC, surface epithelial cells; arrows, luminal expression of NR2B. Scale bars, 20  $\mu\text{m}$  (low-magnification images in A-D) or 100  $\mu\text{m}$  (high magnification image in A).

gastric epithelial cells. NMDA channel activity in brain has long been known to transport  $\text{Ca}^{2+}$  with transport rates dependent on cAMP and protein kinase A (PKA).<sup>22</sup> Furthermore, it is well established that excessive A/A ex-

posure in brain activates NMDA channel activity, resulting in neurotoxicity.<sup>23,29,35</sup> Our results in gastric RGM1 cells in vitro are consistent with these observations. We show that NMDA channel activation by A/A, in particular

NMDA channels with NR2B-containing subunits, rapidly increases intracellular  $\text{Ca}^{2+}$  in a cAMP-dependent manner, which is taken up into the ER and transferred to mitochondria. This large pool of ER  $\text{Ca}^{2+}$  and its inositol-3-phosphate-dependent transfer to mitochondria results in outer mitochondrial membrane damage and ATP depletion, thus reducing epithelial cell viability in the presence of A/A. In addition, we showed that  $\text{Ca}^{2+}$  transcriptionally regulates the expression of cell death effectors and that  $\text{Ca}^{2+}$ -activated calpain and cathepsin B participate in the cytotoxic effects of A/A. Overall, our results provide strong new evidence that A/A cytotoxicity in gastric epithelial cells has a distinct, channel-mediated mechanism that can be blocked with channel inhibitors and, in the continued presence of high levels of A/A, inhibition of NMDA channel activity protects gastric epithelial cells from A/A-induced cell death. Our results also suggest that the majority of vacuoles showed in cells incubated with A/A are dilatations of the ER and not Golgi-derived vacuolar compartments. These novel results provide a new context with which to view the role of A/A in HP infection *in vivo*, and may provide important new insights into HP-induced gastric cancer development.

Apical surface expression of NMDA channels, which we showed to occur in surface epithelial cells from the antrum and corpus *in vivo* and in RGM1 cells *in vitro*, would allow direct access of gastric juice A/A to NMDA channels in these cells. Because we show that wild-type HP expressing *ureB* significantly increases the expression of NR2B subunits *in vitro* and *in vivo*, it is likely that NMDA channel activation in HP infection is greater than in normal mucosa. This result suggests that apoptosis in nontransformed gastric surface cells, which is driven by  $\text{Ca}^{2+}$ -induced mitochondrial dysfunction, may be related directly to the amount of A/A liberated by HP. In addition, surface expression of NMDA channels in gastric cells may constitutively facilitate the ability of dietary amino acids such as glycine and glutamate, which are the NR1 and NR2 channel agonists, respectively, to have a direct effect on the rate of  $\text{Ca}^{2+}$ -influx and thus on cell function and viability. NMDA channel activation by glutamate also may contribute to apoptosis rates in HP infection because gastric juice glutamate levels are increased more than 2-fold in patients with gastritis and nearly 10-fold in HP-infected patients with early gastric cancer.<sup>36</sup>

Although A/A-induced  $\text{Ca}^{2+}$  influx kills gastric epithelial cells in culture, it could be argued that NMDA channel activation early in HP infection serves a protective function *in vivo* by increasing the rate of cell turnover by apoptosis. In primary tumors from patients with gastric cancer, the NR2B subunit of NMDA channels is not expressed owing, in part, to promoter methylation.<sup>24</sup> Determined in a large, pharmacologic unmasking and microarray analysis study, methylation of NR2B was a specific event in gastric cancer, with the highest methylation status in diffuse and intestinal-type gastric cancers.<sup>24</sup> In

addition, NR2B methylation in normal adjacent tissues was suggested to be an important risk factor and molecular marker for tumor formation,<sup>24</sup> suggesting that NR2B normally functions as a tumor suppressor. NR2B promoter methylation, resulting in the significant attenuation of NR2B messenger RNA expression, also occurs in gastric cancer cell lines,<sup>24,30</sup> which we showed in this study to block NR2B protein expression and NMDA-receptor-mediated  $\text{Ca}^{2+}$  permeation in MKN28 cells. We additionally show in RGM1 cells and in MKN28 cells with induced NR2B expression that the effects of A/A are related directly to NMDA channels with NR2B subunit expression. Although it is not known what function NMDA channels provide normally in epithelial cells, studies by others in gastric cancer cells suggest that promoter methylation and down-regulation of the NR2B subunit, in particular, limit apoptosis and cell renewal to enhance cancer progression.<sup>24</sup> The reduction in apoptosis that fosters bacterial persistence later in infection<sup>37</sup> may parallel the timing of NR2B promoter methylation in gastric cells. This interesting possibility should be examined further.

How A/A facilitates NMDA-receptor activation is largely unknown, although it is thought to occur by an A/A-induced depolarization of cell membrane potential, which also occurs with high  $\text{K}^+$ .<sup>23,38</sup> In cultured brain cells, 5 mmol/L  $\text{NH}_4\text{Cl}$  immediately decreased resting membrane potential from  $-96.2$  to  $-89.1$  mV, and 10 and 20 mmol/L  $\text{NH}_4\text{Cl}$  further reduced resting membrane potential to  $-66.3$  and  $-50.4$  mV, respectively.<sup>39</sup> This A/A-induced depolarization of membrane potential is thought to release the  $\text{Mg}^{2+}$  block that normally inhibits channel activity so that  $\text{Ca}^{2+}$  is able to enter cells.<sup>23</sup> This may explain why the sum of fluo-3 and the size of fluo-3-containing vacuoles with A/A exposure in our study were dependent on the A/A concentration. In addition, A/A recently was shown to dose-dependently increase cAMP-PKA levels in cells<sup>40</sup> and Skeberdis et al<sup>22</sup> reported that cAMP-PKA is required to gate NMDA channels in brain. As such, the rate of NMDA-mediated  $\text{Ca}^{2+}$  permeation with A/A exposure also may depend on the level of intracellular cAMP-PKA that is generated. Our results in gastric cells are consistent with this idea because we showed that A/A-induced  $\text{Ca}^{2+}$  permeation is inhibited by cAMP inhibitors and that increasing cAMP with forskolin significantly increased  $\text{Ca}^{2+}$  permeation in the presence of A/A.

Cell signaling pathways involving A/A-induced cAMP-PKA additionally may function in regulating the membrane expression of receptors, thus influencing the rate of  $\text{Ca}^{2+}$  permeation. We show here that NR2B is localized to the cell membrane but in Western blots and in our immunostained images *in vitro* and *in vivo* it is clear that cytoplasmic localization of NR2B also is present. When the NR2A and NR2B subunits of NMDA receptors were transfected into HeLa cells either as heterotetramers or homotetramers, NR2B subunits were associated with Rab11-containing recycling endosomes that were cytoplasmic and played a dominant role in receptor trafficking

to and from the membrane.<sup>41</sup> Roma et al<sup>42</sup> recently showed that both Ca<sup>2+</sup> and cAMP are required to move cytoplasmic recycling endosomes to the surface, suggesting that cAMP generated by A/A may play a role not only in channel gating but in regulating the expression of receptors at the apical surface.

In conclusion, gastric epithelial cells express NMDA channels that, in gastric RGM1 cells, regulate Ca<sup>2+</sup> influx and cell viability in the presence of A/A. Ca<sup>2+</sup> permeation also occurs in a urease-dependent manner in HP-infected MKN28 cancer cells that express active NMDA channels. NMDA channels may play an important pro-apoptotic function in gastric surface epithelial cells, and may prove to be important overall in HP-induced gastric cancer progression by regulating the rate of epithelial cell survival and death.

## Supplementary Material

Note: To access the supplementary material accompanying this article, visit the online version of *Gastroenterology* at [www.gastrojournal.org](http://www.gastrojournal.org), and at doi: [10.1053/j.gastro.2011.08.048](https://doi.org/10.1053/j.gastro.2011.08.048).

## References

1. Parkin DM. The global health burden of infection-associated cancers in the year 2002. *Int J Cancer* 2006;118:3030–3044.
2. Parkin DM, Bray F, Ferlay J, et al. Global cancer statistics, 2002. *CA Cancer J Clin* 2005;55:74–108.
3. Sachs G, Weeks DL, Melchers K, et al. The gastric biology of *Helicobacter pylori*. *Ann Rev Physiol* 2003;65:349–369.
4. Stark RM, Suleiman MS, Hassan IJ, et al. Amino acid utilisation and deamination of glutamine and asparagine by *Helicobacter pylori*. *J Med Microbiol* 1997;46:793–800.
5. Mendz GL, Hazell SL. Amino acid utilization by *Helicobacter pylori*. *Int J Biochem Cell Biol* 1995;27:1085–1093.
6. Leduc D, Gallaud J, Stingl K, et al. Coupled amino acid deamidase-transport systems essential for *Helicobacter pylori* colonization. *Infect Immun* 2010;78:2782–2792.
7. Triebling AT, Korsten MA, Dlugosz JW, et al. Severity of *Helicobacter*-induced gastric injury correlates with gastric juice ammonia. *Dig Dis Sci* 1991;36:1089–1096.
8. Verdu EF, Armstrong D, Sabovcikova L, et al. High concentrations of ammonia, but not volatile amines, in gastric juice of subjects with *Helicobacter pylori* infection. *Helicobacter* 1998;3:97–102.
9. Smoot DT, Mobley HLT, Chippendale GR, et al. *Helicobacter pylori* urease activity is toxic to human gastric epithelial cells. *Infect Immun* 1990;58:1992–1994.
10. Lichtenberger LM, Dial EJ, Romero JJ, et al. Role of luminal ammonia in the development of gastropathy and hypergastrinemia in the rat. *Gastroenterology* 1995;108:320–329.
11. Tsuji M, Kawano S, Tsuji S, et al. Cell kinetics of mucosal atrophy in rat stomach induced by long-term administration of ammonia. *Gastroenterology* 1993;104:796–801.
12. Suzuki H, Yanaka A, Shibahara T, et al. Ammonia-induced apoptosis is accelerated at higher pH in gastric surface cells. *Am J Physiol Gastrointest Liver Physiol* 2002;283:G986–G995.
13. Nakamura E, Hagen SJ. Role of glutamine and arginase in protection against ammonia-induced cell death in gastric epithelial cells. *Am J Physiol Gastrointest Liver Physiol* 2002;283:1264–1275.
14. Hagen SJ, Takahashi S, Jansons R. The role of vacuolation in the death of gastric epithelial cells. *Am J Physiol Cell Physiol* 1997;272:C48–C58.
15. Athmann C, Zeng N, Kang T, et al. Local pH elevation mediated by the intrabacterial urease of *Helicobacter pylori* cocultured with gastric cells. *J Clin Invest* 2000;106:339–347.
16. Boron WF, Waisbren SJ, Bodlin IM, et al. Unique permeability barrier of the apical surface of parietal and chief cells in isolated perfused gastric glands. *J Exp Biol* 1994;196:347–360.
17. Kubota Y, Kato K, Dairaku N, et al. Contribution of glutamine synthetase to ammonia-induced apoptosis in gastric mucosal cells. *Digestion* 2004;69:140–148.
18. Igarashi M, Kitada Y, Yoshiyama H, et al. Ammonia as an accelerator of tumor necrosis factor alpha-induced apoptosis of gastric epithelial cells in *Helicobacter pylori* infection. *Infect Immun* 2001;69:816–821.
19. Wroblewski LE, Shen L, Ogden S, et al. *Helicobacter pylori* dysregulation of gastric epithelial tight junctions by urease-mediated myosin II activation. *Gastroenterology* 2009;136:236–246.
20. Amagase K, Nakamura E, Endo T, et al. New frontiers in gut nutrient sensor research: prophylactic effect of glutamine against *Helicobacter pylori*-induced gastric disease in Mongolian gerbils. *J Pharmacol Sci* 2010;112:25–32.
21. Fernandes HB, Baimbridge KG, Church J, et al. Mitochondrial sensitivity and altered calcium handling underlie enhanced NMDA-induced apoptosis in YAC128 model of Huntington's disease. *J Neurosci* 2007;27:13614–13623.
22. Skeberdis VA, Chevaleyre V, Lau CG, et al. Protein kinase A regulates calcium permeability of NMDA receptors. *Nat Neurosci* 2006;9:501–510.
23. Rodrigo R, Cauli O, Boix J, et al. Role of NMDA receptors in acute liver failure and ammonia toxicity: therapeutic implications. *Neurochem Int* 2009;55:113–118.
24. Liu J-W, Kim MS, Nagpal J, et al. Quantitative hypermethylation of NMDAR2B in human gastric cancer. *Int J Cancer* 2007;121:1994–2000.
25. Hagen SJ, Yang DH, Tashima K, et al. Epithelial cell expression of BCL-2 family proteins predicts mechanisms that regulate *Helicobacter pylori*-induced pathology in the mouse stomach. *Lab Invest* 2008;88:1227–1244.
26. Hagen SJ, Ohtani M, Zhou J-R, et al. Inflammation and foveolar hyperplasia are reduced by supplemental dietary glutamine during *Helicobacter pylori* infection in mice. *J Nutr* 2009;139:912–918.
27. Javitt DC, Frusciante MJ, Zukin SR. Rat brain N-methyl-D-aspartate receptors requires multiple molecules of agonist for activation. *Mol Pharmacol* 1990;37:603–607.
28. Javitt DC, Zukin SR. Biexponential kinetics of [<sup>3</sup>H]MK-801 binding: evidence for access to closed and open N-methyl-D-aspartate receptor channels. *Mol Pharmacol* 1989;35:387–393.
29. Hermenegildo C, Marcaida G, Montoliu C, et al. NMDA receptor antagonists prevent acute ammonia toxicity in mice. *Neurochem Res* 1996;21:1237–1244.
30. Watanabe K, Kanno T, Oshima T, et al. The NMDA receptor NR2A subunit regulates proliferation of MKN45 human gastric cancer cells. *Biochem Biophys Res Commun* 2008;367:487–490.
31. Kim I, Xu W, Reed JC. Cell death and endoplasmic reticulum stress: disease relevance and therapeutic opportunities. *Nat Rev Drug Discov* 2008;7:1013–1030.
32. Hardingham GE. Coupling of the NMDA receptor to neuroprotective and neurodestructive events. *Biochem Soc Trans* 2009;37:1147–1160.
33. Boya P, Kroemer G. Lysosomal membrane permeabilization in cell death. *Oncogene* 2008;27:6434–6451.
34. Goldenring JR, Nam KT, Wang TC, et al. Spasmolytic polypeptide-expressing metaplasia and intestinal metaplasia: time for reevaluation of metaplasias and the origins of gastric cancer. *Gastroenterology* 2010;138:2207–2210.
35. Kosenko E, Llansola M, Montoliu C, et al. Glutamine synthetase activity and glutamine content in brain: modulation by NMDA receptors and nitric oxide. *Neurochem Int* 2003;43:493–499.

36. Nagata Y, Sato T, Enomoto N, et al. High concentrations of D-amino acids in human gastric juice. *Amino Acids* 2007;32:137–140.
37. Mimuro H, Suzuki T, Nagai S, et al. *Helicobacter pylori* dampens gut epithelial self-renewal by inhibiting apoptosis, a bacterial strategy to enhance colonization of the stomach. *Cell Host Microbe* 2007;2:250–263.
38. Sanchez-Perez AM, Llansola M, Cauli O, et al. Modulation of NMDA receptors in the cerebellum: II. Signaling pathways and physiological modulators regulating NMDA receptor function. *Cerebellum* 2005;4:162–170.
39. Allert N, Köller H, Siebler M. Ammonia-induced depolarization of cultured rat cortical astrocytes. *Brain Res* 1998;782:261–270.
40. Svoboda N, Zierler S, Kerschbaum HH. cAMP mediates ammonia-induced programmed cell death in the microglial cell line BV-2. *Eur J Neurosci* 2007;25:2285–2295.
41. Tang TT-T, Badger JD, Roche PA, et al. Novel approach to probe subunit-specific contributions to N-methyl-D-aspartate (NMDA) receptor trafficking reveals a dominant role for NR2B in receptor recycling. *J Biol Chem* 2010;285:20975–20981.
42. Roma JG, Crocenz FA, Mottino AD. Dynamic localization of hepatocellular transporters in health and disease. *World J Gastroenterol* 2008;14:6786–6801.

Received December 3, 2010. Accepted August 29, 2011.

**Reprint requests**

Address requests for reprints to: Susan J. Hagen, PhD, Department of Surgery, E/RW-871, Beth Israel Deaconess Medical Center, 330 Brookline Avenue, Boston, Massachusetts 02215. e-mail: shagen@bidmc.harvard.edu; fax: (617) 975-5562.

**Acknowledgments**

The authors thank Dr Lay-Hong Ang for performing the N-methyl D-aspartate receptor subunit 2B immunostaining, Drs Yi Zheng and Lay-Hong Ang for help with live-cell confocal instrumentation, Dr Zeli Shen for growing *Helicobacter pylori*, and Dr John Woodward for providing the NMDAR2B expression plasmid.

**Conflicts of interest**

The authors disclose no conflicts.

**Funding**

Supported by the National Institutes of Health grants R01DK015681, P30DK037854, and S10RR017927 (S.J.H.); R01DK058587, R01CA77955, and P01116037 (R.M.P.); and R01CA067463 and R01AI/RR037750 (J.G.F.).